

Electrically tunable holographic waveguide display based on holographic polymer dispersed liquid crystal grating

Zhihui Diao (刁志辉)¹, Lingsheng Kong (孔令胜)¹, Junliang Yan (闫俊良)¹,
Junda Guo (郭俊达)¹, Xiaofeng Liu (刘小泮)¹, Li Xuan (宣丽)¹, and Lei Yu (于磊)^{2,*}

¹Changchun Institute of Optics, Fine Mechanics and Physics, Chinese Academy of Sciences, Changchun 130033, China

²Anhui Institute of Optics and Fine Mechanics, Chinese Academy of Sciences, Hefei 230031, China

*Corresponding author: yulei@aiofm.ac.cn

Received August 14, 2018; accepted November 12, 2018; posted online December 25, 2018

In this Letter, we present an electrically tunable holographic waveguide display (HWD) based on two slanted holographic polymer dispersed liquid crystal (HPDLC) gratings. Experimental results show that a see-through effect is obtained in the HWD that both the display light from HWD and the ambient light can be clearly seen simultaneously. By applying an external electric field, the output intensity of the display light can be modulated, which is attributed to the field-induced rotation of the liquid crystal molecules in the two HPDLC gratings. We also show that this electrically tunable performance enables the HWD to adapt to different ambient light conditions. This study provides some ideas towards the development of HWD and its application in augmented reality.

OCIS codes: 230.3720, 160.3710, 050.1950, 090.2890.

doi: 10.3788/COL201917.012301.

Recently, augmented reality (AR) has become a hot research topic, as it can build a bridge between the virtual world and real world, which enables people to obtain virtual information while being immersed in the real environment^[1,2]. As the key display element in AR, holographic waveguide display (HWD) based on volume holographic gratings has attracted a great deal of interest, since it shows some advantages of high see-through transmittance, small size, light weight, and low cost, which is suitable for near-eye display^[3,4]. Many researchers have done excellent work on HWD to improve its display characteristics, such as full-color display^[5,6], color uniformity optimization^[7,8], field of view enlargement^[9], exit pupil expansion^[10,11], and efficiency improvement^[12,13]. Among these reports, however, no report has been devoted to solving the problem that is the intensity mismatch between the display light of virtual information and the ambient light of the real environment. It is well known that the display light generated by a micro-display source always has a more stable intensity compared to the variable ambient light^[3,4]. When the ambient light darkens (e.g., driving a car into a tunnel from open-air), the display light would become relatively stronger for the human eyes. The excessive intensity contrast ratio between display light and ambient light would not only reduce the merging effect between virtual information and real environment, but also lead to viewing fatigue or even serious visual discomfort, such as headaches^[14]. Similarly, when the ambient light brightens, the display light would become relatively weaker so that the people can hardly recognize the virtual information. Therefore, the intensity mismatch between display light and ambient light will be a serious problem that limits the application of HWD in AR.

In this Letter, to solve that problem, we present an electrically tunable HWD based on two slanted holographic polymer dispersed liquid crystal (HPDLC) gratings, which are utilized to couple in and couple out the display light, respectively. The HPDLC grating, formed by photopolymerization-induced phase separation^[15–17], has the merits of ease of fabrication, rapid and large-area prototyping, low cost, and electrically tunable capability^[18]. The diffraction efficiency of the HPDLC grating can be tuned under the electric field^[15], because the liquid crystal (LC) molecules in the grating are electro-optical birefringent materials, and their refractive indices can be changed due to the field-induced rotation^[19]. In the HWD, the output intensity of the display light is highly dependent on the diffraction efficiency of the grating^[3,12], so the tunable HPDLC grating provides a method to modulate the display light. Experimental results show that when the input intensity of the display light is fixed at 374 μW , the output intensity can be modulated from 199 to 9 μW by increasing the external electric field. During the modulation process, no optical apparatuses are moved or altered, but only the electric field is changed. Therefore, the output intensity of the display light from the HWD can be modulated actively and simply according to the variance of the ambient light, and then the intensity mismatch problem can be solved. It should be noted that the HPDLC grating has been used to fabricate the HWD previously^[20], but the electrically tunable performance of HWD and its tuning mechanism have not been investigated. Therefore, this Letter is the first time, to the best of our knowledge, that an electrically tunable HWD is presented, showing its potential to improve the environmental adaptability of HWD.

Figure 1 shows the fabrication process of the proposed HWD. Two indium tin oxide (ITO)-coated glasses were

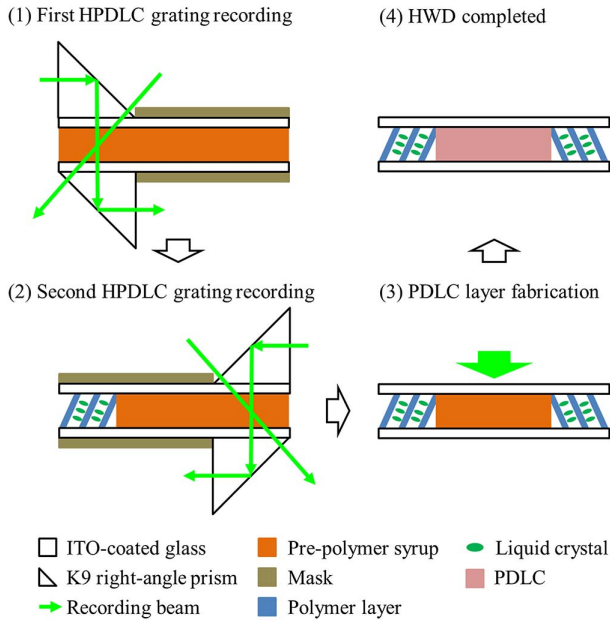


Fig. 1. Fabrication process of the proposed HWD.

combined to form a sample cell, where the cell gap was controlled by Mylar spacers at $10\ \mu\text{m}$. The thicknesses of the glass substrate and ITO layer were $1\ \text{mm}$ and $30\ \text{nm}$, respectively, and the refractive index of the glass substrate was 1.516 . Then, a uniform mixture of the HPDLC pre-polymer syrup, composed of nematic LC TEB30A ($n_o = 1.522$, $n_e = 1.692$, $33.0\ \text{wt.}\%$, Slichem), acrylate monomer phthalic diglycol diacrylate (PDDA, $54.6\ \text{wt.}\%$, Sigma-Aldrich), and photo-initiators ($12.4\ \text{wt.}\%$), was injected into the sample cell via capillary action in the dark. The refractive index of the pure polymer formed by monomer PDDA was 1.525 measured by an Abbe refractometer. The detailed material composition of the photo-initiators can be found elsewhere^[21]. To ensure the diffracted light through grating can be totally reflected off the air-glass interfaces and propagate in the waveguide, two K9 right-angle prisms were used here to fabricate the slanted HPDLC grating^[20,22]. Two coherent recording beams from a $532\ \text{nm}$ neodymium-doped yttrium aluminum garnet (Nd:YAG) laser were directed perpendicularly on the hypotenuse and one leg of the upper prism, respectively. Considering that the pre-polymer syrup had a similar refractive index to the glass substrate and prism, the angle of the two recording beams in the pre-polymer syrup was about 45° . Therefore, a slanted HPDLC grating with a period of $455\ \text{nm}$ and slanted angle of 22.5° with respect to the normal of the glass substrate can be achieved after exposure. The obtained HPDLC grating was composed of alternating polymer and LC layers^[15]. In addition, the lower prism was used to avoid the trapping of the recording beam due to the total internal reflection (TIR) on the glass substrate, and the refractive index matching oil was used to fill up the air gap between the glass substrates and prisms. During the exposure process, two masks were used to

cover the unrelated area. When the first grating was done, the second grating was recorded in the other end of the sample cell by mirror operation. After recording the two gratings, the sample cell was exposed to a single recording beam to form a polymer dispersed LC (PDLC) layer between the two gratings. The PDLC had homogeneous optical characteristics^[23], and its refractive index was 1.543 measured by an Abbe refractometer. The scattering loss of the PDLC layer was also measured to be only 5% , which was attributed to the small thickness and low LC concentration ($33\ \text{wt.}\%$), so the scattering effect of the PDLC would not have significant impact on HWD performance. Finally, the HWD based on two slanted HPDLC gratings was obtained. It should be noted that the structure of this proposed HWD is a little different from the one of a conventional HWD^[3], because the two slanted HPDLC gratings need to be kept in the sample cell that can provide a vacuum environment to fix the flowable LC molecules. Moreover, the waveguide core layer is composed of two glass substrates and one PDLC layer. Although the composition is complex, the small thickness of the PDLC layer and the similar refractive index between the glass substrate and PDLC layer can ensure that there is efficient light propagation in the waveguide core layer.

To determine the LC molecules orientation in the slanted HPDLC grating, which was crucial to the electrically tunable performance of the HWD, the diffraction efficiency of the grating under different polarization states was measured, as shown in Fig. 2(a). A combination of a spatial filter and collimated lens was used to expand the laser beam from a $532\ \text{nm}$ Nd:YAG laser into a collimated light, which was then directed perpendicularly on the

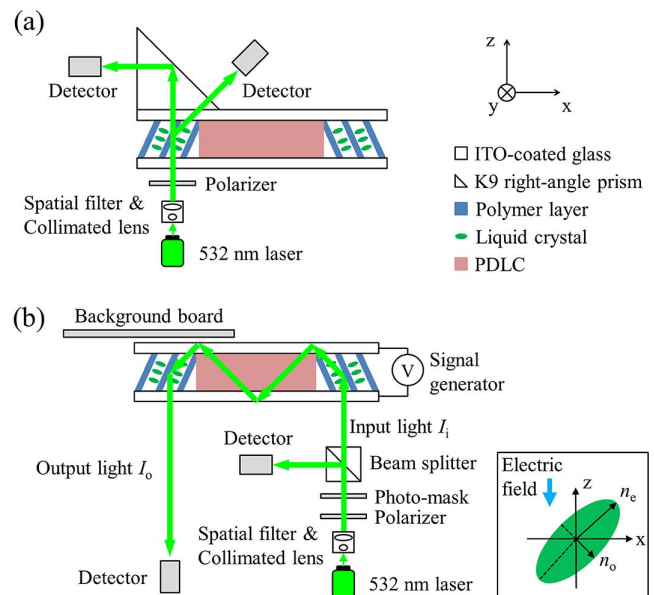


Fig. 2. Experimental setups to (a) measure the diffraction efficiency of the slanted HPDLC grating and (b) test the electrically tunable performance of the HWD. The inset in (b) shows the orientation of the LC molecule under an electric field.

sample cell. The laser polarization state was modulated by a polarizer, in which the polarizer angle of 0° corresponded to the s polarization, which was parallel to the y axis, and 90° corresponded to the p polarization, which was parallel to the x axis. A K9 right-angle prism was used to lead out the diffracted light. By measuring the intensities of the transmitted and diffracted lights, respectively, the diffraction efficiency of the slanted HPDLC grating can be obtained. Considering that the two gratings were mirror symmetrical, measuring one grating was enough.

Figure 2(b) shows the experimental setup to test the electrically tunable performance of the HWD. A 532 nm Nd:YAG laser was used as a display source. The laser beam was expanded into a collimated light by a combination of a spatial filter and collimated lens and directed perpendicularly on the sample cell. The sizes of the HPDLC grating and PDLC film were measured to be $13 \text{ mm} \times 20 \text{ mm}$ and $6 \text{ mm} \times 20 \text{ mm}$, respectively. A photo-mask with a designed pattern was placed in the light path to generate an input image by modulating the shape of the collimated light, which can be seen as a simplified method to simulate the image generation process of LC on silicon (LCoS)^[24]. The first slanted HPDLC grating coupled the display light of the input image into the waveguide in a TIR condition because the diffracted light had a propagation angle of 45° with respect to the normal of the glass substrate, which was beyond the TIR critical angle of 41.3° [$\arcsin(1/1.516)$]. After several times of TIR, the display light was coupled out by the second slanted HPDLC grating. A background board was placed behind the out-coupled HPDLC grating region to test the see-through effect of the HWD. The input and output intensities of the display light were detected by two detectors and labeled as I_i and I_o , respectively. In order to enable the electrical modulation of the HWD, a square-wave voltage of 1 kHz frequency was output by a signal generator and applied on the sample cell.

Figure 3 shows the diffraction efficiency of the slanted HPDLC grating as a function of the polarizer angle, in which 0° (180°) and 90° correspond to s polarization and p polarization, respectively. It can be seen that when the probe light turns from s polarization to p polarization, the diffraction efficiency increases gradually, and the highest value of 82.8% is achieved at the polarizer angle of 90° . This polarization-dependent performance is attributed to the LC molecules orientation in the HPDLC grating under the anchoring effect of polymer filaments^[25]. In our material system, the refractive index of pure polymer n_p (1.525) is much closer to n_o (1.522) rather than n_e (1.692); so, if the polarization state of the probe light is more parallel to the long axis of the LC molecule, then a higher refractive index modulation Δn of the grating can be obtained. Moreover, according to the coupled-wave theory for the volume holographic grating^[26], a higher Δn can lead to a higher diffraction efficiency. Therefore, on the basis of the above analysis and the experimental results shown in Fig. 3, it can be concluded that the LC molecules orientations in the two slanted HPDLC gratings are

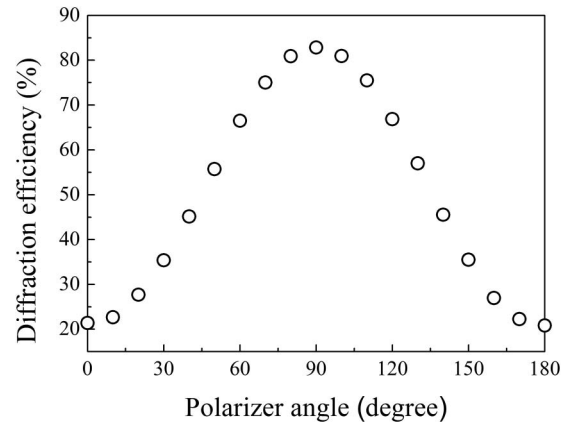


Fig. 3. Diffraction efficiency of the slanted HPDLC grating as a function of polarizer angle. 0° and 180° correspond to s polarization; 90° corresponds to p polarization.

preferentially parallel to the grating vector [Fig. 2(a)], which is in good agreement with previous reports^[25,27].

After determining the LC molecules orientation in the slanted HPDLC gratings, a preliminary test of the HWD was performed with no electric field applied. To ensure that the two gratings have the highest diffraction efficiencies, the display source (532 nm collimated Nd:YAG laser) was set to be p polarized. The pattern of the photo-mask was chosen to be the Arabic numeral “7”, whose size was measured to be $3 \text{ mm} \times 4 \text{ mm}$. The display light carrying the information from the photo-mask was directed perpendicularly on the first grating and coupled into the waveguide. After several times of TIR, the display light was coupled out by the second grating and captured by a camera, as shown in Fig. 4. The green Arabic numeral “7” is the display image that is produced by the display source after passing through the HWD, and the white board with black texts “ $3 + 4 =$ ” is the background content. Through the out-coupled HPDLC grating region, both the display image and the background content can be easily distinguished and clearly seen simultaneously, showing a good see-through effect of the HWD. The size of the display image is measured to be about $3.5 \text{ mm} \times 4.6 \text{ mm}$, which is a little bigger than the

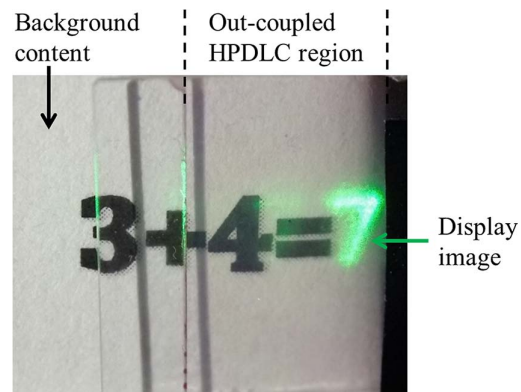


Fig. 4. Display image of HWD and the background content.

photo-mask size, because the display image has some blur, which is caused by the surface unevenness between the holographic material and glass substrates^[28]. Moreover, the intensities of the input light I_i and output light I_o are measured to be 374 and 199 μW , respectively, which indicates that the system efficiency of the HWD is about 53.2%.

A further experiment was carried out to investigate the electrically tunable performance of the HWD by applying an electric field on the sample cell. The output intensity I_o under different electric fields was detected and shown in Fig. 5(a), in which the input intensity I_i was kept constant at 374 μW for all electric fields. It can be seen that when increasing the electric field from 0 to 17 $\text{V}/\mu\text{m}$, the output intensity I_o can be controlled to decrease from 199 to 9 μW . This electrically tunable performance is attributed to the field-induced rotation of LC molecules in the two slanted HPDLC gratings. Figure 5(b) shows the diffraction efficiency of the slanted HPDLC grating under different electric fields. It can be found that the diffraction efficiency decreases with the increasing electric field. Upon application of an electric field, LC molecules tend to align with their long axes into the field direction along the z axis and rotate in the x - z plane [the inset in Fig. 2(b)]. Such rotation of LC molecules will decrease their effective

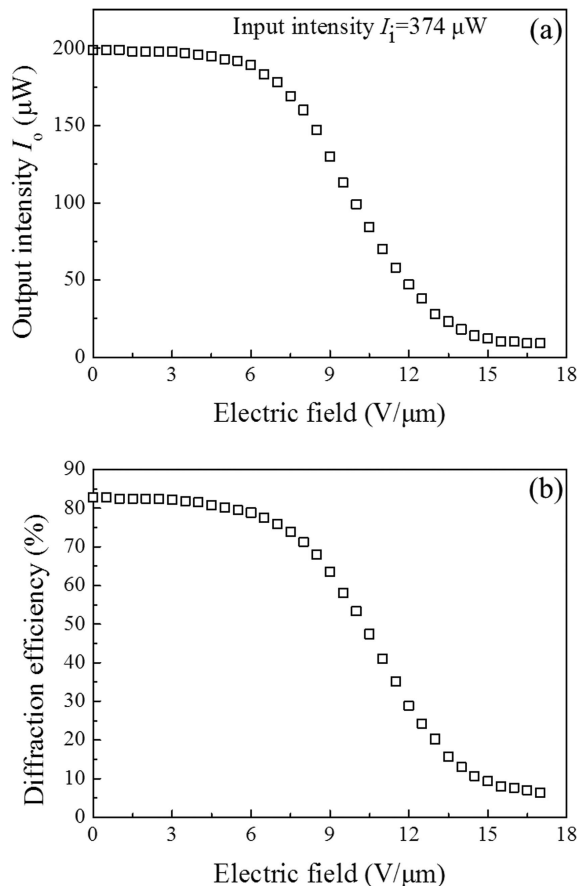


Fig. 5. (a) Output intensity I_o under different electric fields. (b) Diffraction efficiency of the slanted HPDLC grating under different electric fields.

refractive indices for the p-polarized display light (polarization state along the x axis) and reduce the Δn of the grating. Then, the reduced Δn will lead to a lower diffraction efficiency of the grating^[26] and thus a lower output intensity of the display light from HWD. It should be noted that the driving electrical field, as shown in Fig. 5(a), may be a little higher when considering the practical application. To further reduce the electric field, the HPDLC grating can be recorded by introducing surfactant^[29] or fluorine-substituted monomer^[30].

Moreover, by adjusting the ambient light, we will show how the electrically tunable performance of the HWD solves the intensity mismatch problem between the display light and ambient light. Figure 6(a) shows the display effect of the HWD under a high ambient light condition while no electric field is applied. The display image (green Arabic numeral “7”) and the background content (white board with black texts “3 + 4 =”) can be clearly seen simultaneously. Then, the ambient light is turned down, as shown in Fig. 6(b), and the display light becomes relatively brighter compared to the weak ambient light. Actually, when we looked at the display image of the HWD directly by the naked eye in the experiment, the excessive intensity contrast ratio between the display light and ambient light leads to a dazzling viewing experience, and the background content was hard to distinguish. To improve the display effect of the HWD, an electric field of 10 $\text{V}/\mu\text{m}$ is applied to the sample cell to modulate the display light, and the result is shown in Fig. 6(c). It can be seen that the display light is decreased to an acceptable intensity compared to the ambient light, which makes the HWD suitable for watching. Therefore, as expected, the intensity mismatch problem can be efficiently solved because the display light intensity of the HWD can be modulated electrically according to the variable ambient light. Moreover, it should be noted that two green Arabic numerals “7” can be seen in Fig. 6(b), in which the left one is with low brightness. This left “7” is generated by the beam expander effect of the grating in the HWD^[10,11], which can be easily removed by controlling the dimension of the out-coupled HPDLC grating region in the sample cell.

In conclusion, we have demonstrated an electrically tunable HWD based on two slanted HPDLC gratings. By determining the LC molecules orientation in the two gratings, the electrically tunable performance of the HWD is investigated in detail. Experimental results show

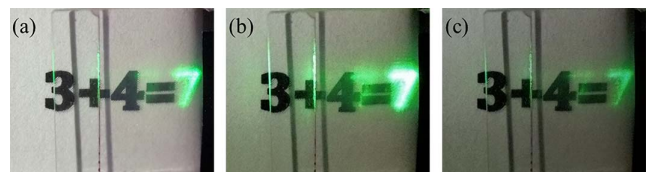


Fig. 6. Display effect of the HWD under different ambient light and electric fields. (a) High ambient light and 0 $\text{V}/\mu\text{m}$; (b) low ambient light and 0 $\text{V}/\mu\text{m}$; (c) low ambient light and 10 $\text{V}/\mu\text{m}$.

that the output intensity of the display light from HWD can be decreased by increasing the external electric field, which is attributed to the field-induced rotation of the LC molecules in the two HPDLC gratings. This electrically tunable performance can enable the HWD to modulate its display light intensity according to the variable ambient light, which ensures an intensity balance between the two lights and makes the HWD suitable for watching under different ambient light conditions. In our further work, an embedded ambient light sensor will be introduced in the HWD, so the display light intensity of HWD can be controlled adaptively according to the variable ambient light, which leads to fully automatic modulation. Therefore, we believe the active optical device HPDLC grating will open a promising way to design HWD and broaden its applications in the field of AR.

This work was supported by the Youth Innovation Promotion Association, Chinese Academy of Sciences (Nos. 2018251 and 2017264) and the National Natural Science Foundation of China (Nos. 11704378 and 61705221).

References

1. T. Sielhorst, M. Feuerstein, and N. Navab, *J. Disp. Technol.* **4**, 451 (2008).
2. X. D. Hu and H. Hua, *Opt. Express* **22**, 13896 (2014).
3. B. Kress and T. Starner, *Proc. SPIE* **8720**, 87200A (2013).
4. J. P. Rolland, K. P. Thompson, H. Urey, and M. Thomas, *Handbook of Visual Display Technology*, J. Chen, W. Cranton, and M. Fihn, eds. (Springer, 2012), p. 2145.
5. H. Mukawa, K. Akutsu, I. Matsumura, S. Nakano, T. Yoshida, M. Kuwahara, K. Aiki, and M. Ogawa, *SID Int. Symp. Dig. Tech. Pap.* **39**, 89 (2008).
6. J. A. Piao, G. Li, M. L. Piao, and N. Kim, *J. Opt. Soc. Korea* **17**, 242 (2013).
7. M. L. Piao and N. Kim, *Appl. Opt.* **53**, 2180 (2014).
8. Z. Shen, Y. Zhang, Y. Weng, and X. Li, *SID Int. Symp. Dig. Tech. Pap.* **48**, 1634 (2017).
9. J. Han, J. Liu, X. C. Yao, and Y. T. Wang, *Opt. Express* **23**, 3534 (2015).
10. A. Cameron, *Proc. SPIE* **8383**, 83830E (2012).
11. N. N. Zhang, J. Liu, Z. M. Wu, R. Shi, and Y. T. Wang, *SID Int. Symp. Dig. Tech. Pap.* **45**, 668 (2014).
12. N. N. Zhang, J. Liu, J. Han, X. Li, F. Yang, X. G. Wang, B. Hu, and Y. T. Wang, *Appl. Opt.* **54**, 3645 (2015).
13. C. Neipp, J. Frances, F. J. Martinez, R. Fernandez, M. L. Alvarez, S. Bleda, M. Ortuno, and S. Gallego, *Polymers* **9**, 395 (2017).
14. D. A. Atchison and G. Smith, *Optics of the Human Eye* (Elsevier, 2000).
15. T. J. Bunning, L. V. Natarajan, V. P. Tondiglia, and R. L. Sutherland, *Annu. Rev. Mater. Sci.* **30**, 83 (2000).
16. Z. Diao, L. Xuan, L. Liu, M. Xia, L. Hu, Y. Liu, and J. Ma, *J. Mater. Chem. C* **2**, 6177 (2014).
17. R. Caputo, L. De Sio, A. Veltri, and C. Umerton, *Opt. Lett.* **29**, 1261 (2004).
18. Z. Diao, L. Kong, L. Xuan, and J. Ma, *Org. Electron.* **27**, 101 (2015).
19. D. K. Yang and S. T. Wu, *Fundamentals of Liquid Crystal Devices*, 2nd ed. (Wiley, 2014).
20. H. T. Dai and X. W. Sun, *SID Int. Symp. Dig. Tech. Pap.* **42**, 1238 (2011).
21. Z. Diao, W. Huang, Z. Peng, Q. Mu, Y. Liu, J. Ma, and L. Xuan, *Liq. Cryst.* **41**, 239 (2014).
22. J. Qi, M. E. Sousa, and G. P. Crawford, *Mol. Cryst. Liq. Cryst.* **433**, 267 (2005).
23. M. Liu, Y. Liu, G. Zhang, L. Liu, Z. Diao, C. Yang, Z. Peng, L. Yao, J. Ma, and L. Xuan, *Liq. Cryst.* **43**, 417 (2016).
24. S. Liu, P. Sun, C. Wang, and Z. Zheng, *Opt. Commun.* **403**, 376 (2017).
25. W. Huang, Y. Liu, Z. Diao, C. Yang, L. Yao, J. Ma, and L. Xuan, *Appl. Opt.* **51**, 4013 (2012).
26. H. Kogelnik, *Bell Syst. Tech. J.* **48**, 2909 (1969).
27. C. M. Van Heesch, H. Jagt, C. Sanchez, H. J. Cornelissen, D. J. Broer, and C. W. M. Bastiaansen, *Chem. Rec.* **5**, 59 (2005).
28. R. Shi, J. Liu, H. Zhao, Z. Wu, Y. Liu, Y. Hu, Y. Chen, J. Xie, and Y. Wang, *Appl. Opt.* **51**, 4703 (2012).
29. Y. J. Liu, X. W. Sun, H. T. Dai, J. H. Liu, and K. S. Xu, *Opt. Mater.* **27**, 1451 (2005).
30. Z. Zheng, J. Ma, W. Li, J. Song, Y. Liu, and L. Xuan, *Liq. Cryst.* **35**, 885 (2008).